

An Antibacterial Submicron Fiber Mat with *In Situ* Synthesized Silver Nanoparticles

Pedro J. Rivero,¹ Aitor Urrutia,¹ Javier Goicoechea,¹ Yoany Rodríguez,² Jesús M. Corres,¹ Francisco J. Arregui,¹ Ignacio R. Matías¹

¹Nanostructured Optical Devices Laboratory, Electric and Electronic Engineering Department, Public University of Navarra, Edif. Los Tejos, Campus Arrosadía, 31006, Pamplona, Spain

²Telecommunications Department, Pinar del Río University, Av. Martí 270, Pinar del Río, Cuba

Received 29 July 2011; accepted 26 January 2012

DOI 10.1002/app.36886

Published online in Wiley Online Library (wileyonlinelibrary.com).

ABSTRACT: This work presents an alternative approach for fabricating electrospun submicron highly hydrophilic fiber mats loaded with silver nanoparticles. These fiber mats show a high efficient antibacterial behavior, very attractive for applications like wound healing and skin regeneration processes. The fabrication method is divided in two steps. First, poly(acrylic acid) (PAA) and β -cyclodextrin (β -CD) submicron fibers were electrospun and further stabilized using a thermal treatment, yielding stable hydrogel-like fibers with diameters ranging from 100 nm up to several microns. In the second step, silver ions were loaded into the fibers and then reduced to silver nanoparticles *in-situ*. The electrospinning parameters were adjusted to achieve the

desired properties of the fiber mat (density, size) and afterwards, the characteristics of the silver nanoparticles (amount, size, aggregation) were tuned by controlling the silver ion loading mechanism. Highly biocide surfaces were achieved showing more than 99.99% of killing efficiency. The two-step process improves the reproducibility and tunability of the fiber mats. To our knowledge, this is the first time that stable hydrogel fibers with a highly biocide behavior have been fabricated using electrospinning. © 2012 Wiley Periodicals, Inc. *J Appl Polym Sci* 000: 000–000, 2012

Key words: electrospinning; hydrogel; silver nanoparticles; *in situ* synthesis

INTRODUCTION

Microbes and bacteria are the most abundant of all living organisms and a large number of them are pathogens and disease-causing organisms. Because of this there is a high concern in preventing the emergence of germs in products which are directly or indirectly used by humans. Consequently, to avoid the apparition of these microorganisms in instrumentals, devices, laboratories, or operating rooms, there is an enormous interest in the research of highly efficient and low cost antibacterial surface treatments and coatings.^{1,2}

It is well known that silver is considered a very good antibacterial agent and silver ions show a notorious broad spectrum biocide effect. In fact, there are numerous research works that use silver nanoparticles to obtain highly antibacterial surfaces.^{3–6} Moreover, silver is particularly attractive because combines this high toxicity for bacteria with a low

toxicity for humans.^{7–9} Its disinfectant properties for hygienic and medicinal purposes are known since ancient times and, for example, silver was extensively used to prevent wound infection during the World War I.¹⁰

Most of the approaches for achieving antibacterial surfaces are based on doping some elements with silver particles which act as a silver ion source, for example in textiles,^{11,12} surgical instruments,¹³ and other surfaces.¹⁴ However, the biocide efficiency of such coatings depends on the ability of the trapped silver to release ions. Consequently, silver particles with a high specific surface area show more efficient ion release mechanisms and therefore the antibacterial effect is enhanced. Recently, the use of nanotechnology has made possible the fabrication of new nanostructured materials with an extremely high specific surface area. This remarkable property can significantly improve the antibacterial efficiency of such coatings. Nanotechnology also offers the additional possibility of tuning the overall properties of the coating by properly designing the composition and morphology of the films, opening the door to the combination of the biocide effect with other desired properties (optical, mechanical, etc.)

Some authors have reported that silver nanoparticles,¹⁵ nanorods,¹⁶ or nanotubes¹⁷ are especially efficient antibacterial agents because of their large

Correspondence to: A. Urrutia (aitor.urrutia@unavarra.es).

Contract grant sponsors: Spanish Ministry of Education and Science, CICYT-FEDER TEC2010-17805, Fuentes Dutor Foundation research grant (COINA).

surface to volume ratio. In the most usual approach, such silver nanoparticles have been immobilized on inorganic porous hosts such as zeolites, calcium phosphate, and carbon fiber.^{18–20} Moreover, silver-supported silica materials, such as silica glass,²¹ silica thin films,²² and silica nanoparticles,²³ are also good candidates for antibacterial materials due to their fine chemical durability and high antibacterial activity.

A good alternative to fabricate materials with high specific surface is the electrospinning technique. Using this technique, continuous ultrathin polymeric fibers can be fabricated. Schematically the electrospinning technique can be described as follows, when a high voltage is applied to a polymeric solution with respect to a grounded electrode, the polymeric solution becomes charged and, due to electrostatic attraction, a stream of liquid erupts from the surface, and is launched towards the grounded electrode where the substrate to be coated is placed. If the molecular cohesion of the solution is sufficiently high, a continuous thin fiber is formed and elongated following the electrical field direction. Simultaneously, the solvent is evaporated during the flight of the fiber and this nanofiber is finally deposited on the collector (substrate). The thinning of the fiber leads to the fabrication of filaments up to several tens of nanometers in diameter that superpose randomly forming a fiber web.²⁴ These fibrous membranes obtained using electrospinning technique have a strong potential application in sensors and other fields where a very large specific surface area is needed, such as in the fabrication of antimicrobial surfaces. Such fiber mats may have a specific surface area of approximately one to two orders of magnitude larger than the specific surface area of continuous flat films,²⁵ boosting the efficiency of the desired device.

In this work, poly(acrylic acid) PAA has been used as the polymer to create the fibrous membranes onto glass substrates. Afterward, those fibers were used as hosts for the *in situ* synthesis of silver nanoparticles. The combined effect of the nanoparticle distribution together with the fibrous nature of the electrospun mat enhances the efficiency of the coating and allows good antibacterial behaviors with very small amounts of silver. Most of the previous works include the silver in the polymeric precursor solution before the electrospinning process is carried out, in the form of AgNO_3 ,^{26–29} or directly as metallic nanoparticles.^{30,31} In such approaches the fibers are electrospun already including the silver particles within and the characteristics of the final fiber mat completely depend on the composition of the spinning solution. Nevertheless, in this work, an alternative approach is studied. Instead of projecting the silver nanoparticles embedded in the polymer fibers,

chemically stable polymer-only fibers were spun and the silver was loaded into the fibers in a latter step using an *in situ* reduction method. To achieve optimized antibacterial coatings, the fiber mats characteristics (size, density) are adjusted with the electrospinning parameters and afterwards, the silver nanoparticle characteristics are tuned by means of adjusting their particle loading properties (amount, size, and aggregation).

EXPERIMENTAL METHODS

Materials

The polymers poly(acrylic acid), PAA ($M_w \approx 100.000$ sol. 35 wt % in water), and β -cyclodextrin, β -CD (purity 98%) were provided from Sigma-Aldrich. Silver nitrate, AgNO_3 (>99% titration) and dimethylamine borane (DMAB) (97%) were also purchased from Sigma Aldrich. All chemicals were used without any further purification.

Lactobacillus plantarum stock culture (CECT #4005) was obtained from CECT (The Spanish Type Culture Collection, University of Valencia). Tryptic Soy Broth (TSB) and Tryptic Soy Agar were also provided from Sigma Aldrich.

Electrospinning of the fibers

The polymeric solution concentration was varied to get different diameter fibers. A concentration of 10 wt % of PAA was used for the thicker fibers, while a 5 wt % of PAA was used for the thinner ones. The solutions were prepared using ultrapure water (18.2 $\text{M}\Omega\cdot\text{cm}$). Different amounts of the crosslinker agent β -CD were added to the PAA solutions to get a 20% of β -CD/PAA weight ratio. Once the polymeric solution was prepared, it was immediately used in the electrospinning process. The solution flux is fixed to 1 mL/h using a syringe pump. The needle (anode) and an aluminum sheet (cathode) were placed 25 cm one from the other, and a voltage of 13.5 kV was applied between them. Glass substrates were placed on the aluminum cathode in order to collect the electrospun fibers. In Figure 1, it is observable the typical Taylor cone formed at the needle,^{32,33} and a picture of the fibers being electrospun.

Silver nanoparticle synthesis

After the fibers have been crosslinked then the silver nanoparticles (NPs) were synthesized within the fibers. The fiber mats were immersed into a silver nitrate 0.1M solution for 5 min in order to load the available carboxylic groups of the PAA with Ag^+ via ion interchange.^{34,35} Then, the samples were rinsed in ultrapure water and the Ag^+ ions loaded

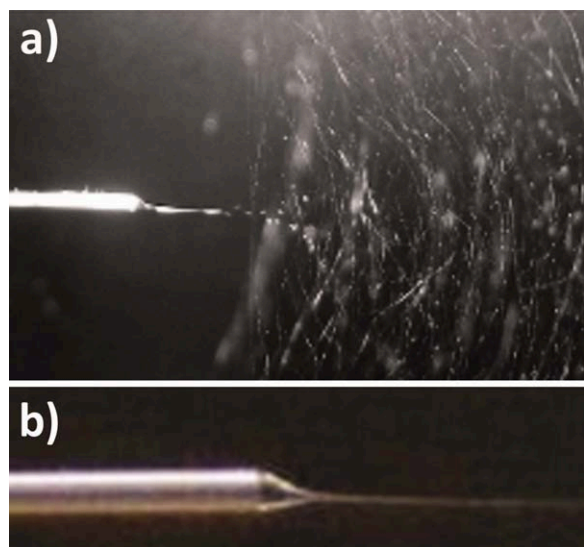


Figure 1 Pictures of the PAA+ β -CD fibers during the electrospinning process. a) shows the needle (left) and the fibers being electrospun towards the cathode (right). b) Detailed view of the Taylor cone formed at the tip of the needle. [Color figure can be viewed in the online issue, which is available at wileyonlinelibrary.com.]

into the fibers were reduced to Ag⁰ by immersing the samples into a 0.1M dimethylamine borane (DMAB) water solution which acts as a reducing agent.

Fiber characterization

The fiber mats were characterized morphologically using optical microscopy (Leica DM2500P) and atomic force microscopy (AFM), (Innova, Veeco) working in tapping mode. Scanning electron microscopy (SEM), (UltraPlus FESEM, Carl Zeiss) was used to improve the characterization of the fibers. Ag nanoparticles were characterized by transmission electron microscopy (TEM), (Carl Zeiss Libra 120). Samples for TEM were prepared by dropping and evaporating the suspensions onto a collodion-coated copper grid. The optical properties of the fibrous coatings were measured by UV-VIS spectrometry (Jasco V-630).

Bacteriological test method

The antibacterial activity of the new coatings against the *L. plantarum* bacteria was assessed by a viable cell-counting method.³⁶ *L. plantarum* was inoculated in a Tryptic Soy Broth aqueous medium and incubated at 37°C for 24 h. The obtained bacterial suspension had $\sim 4.8 \cdot 10^8$ CFU/mL.

The bacterial suspension was shaken and diluted 10^6 times. "Tryptic Soy Agar" was autoclaved at 121°C for 30 min and cooled in sterile Petri-dishes to form a 3 mm thick slab. Then 0.1 mL bacterial

suspension dilution was spread uniformly on the surface of the nutrient agar slab. The substrates coated with Ag NPs loaded electrospun fiber mats were then placed onto the agar slab. Bare glass slides were also placed as reference (previously disinfected by dipping in isopropyl alcohol and treated by contact flame) by the same way. Then, Petri-dishes were introduced into an incubator for 24 h at 37°C and the colonies were counted.

RESULTS AND DISCUSSION

In this work, the fabrication technique is based on the creation of fibers by the application of a traction force to a polymeric solution. This tensile force is created by a strong electrical field which accelerates the polymer towards a cathode. If the cohesive forces inside the polymeric solution are high enough, the electrical projection of the solution will give a polymer fiber, which is accelerated towards the cathode. There are several parameters that play a key role in the final fiber properties, such as the polymer concentration, solvent, temperature, distance, voltage, etc. More detailed description of the electrospinning technique can be found elsewhere.^{32,33}

Once the electrospinning process is completed, the fiber mats were thermally treated at 140°C for 30 min. These fibers were cured in order to achieve a chemical stabilization of the polymer with the formation of ester bonds in the final structure of our fiber mat (see Fig. 2). This reaction has a first step of dehydration of the carboxylic groups of PAA giving glutaric anhydride-like rings. These anhydride rings can interact with the hydroxyl terminations of the β -CD giving a covalent bond between the PAA and the β -CD. As far as the β -CD rings have several OH terminations, one cycle can result chemically bonded to more than one PAA polymeric chain, acting as crosslinker.

In Figure 3, the FTIR spectra of two different electrospun fibers are shown. The first one consists in only PAA electrospun fibers and the other sample consists in PAA+ β -CD electrospun fibers thermally treated at 140°C for 30 min (coded as PAA+ β -CD+ Δ T). The use of β -CD as a crosslinker in aqueous PAA solution produces ester bonds by esterification process.³⁷ The transmission FTIR spectrum of crosslinked electrospun fibers shows absorption bands characteristics of such ester bonds. More specifically, a strong absorption band in the 1750–1700 cm^{-1} region is attributed to the ester carbonyls and also to the carboxylic carbonyl bonds, present both in the free carboxylic acid groups of PAA and also in the β -CD-PAA ester bonds. Moreover, the bands in the 1300–1100 cm^{-1} region are attributed to the C–O stretching vibrations of carboxylic and ester functional groups, and such bands are stronger in

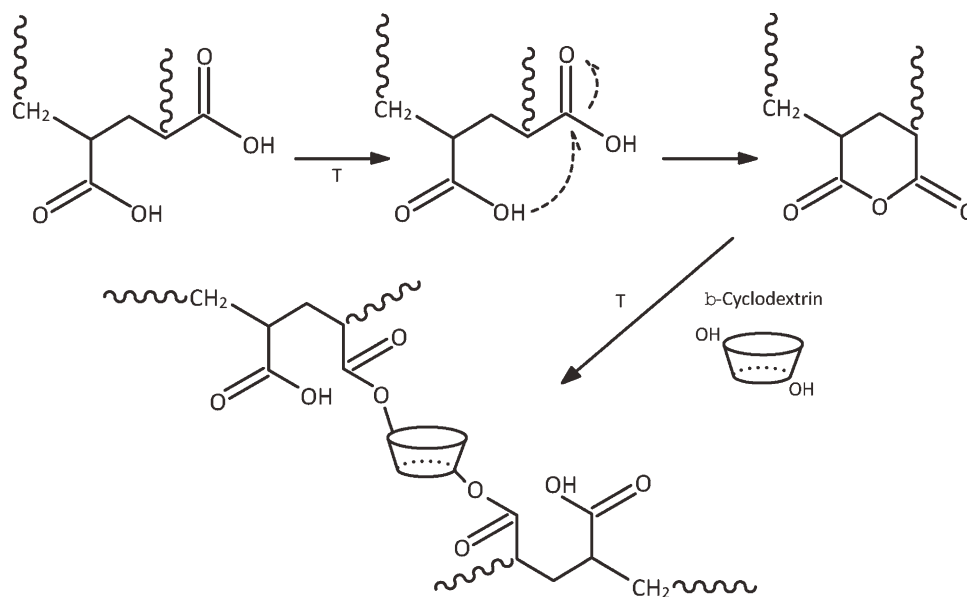


Figure 2 Crosslink reaction scheme of the thermally-treated electrospun nanofibers.

the crosslinked fibers than in the crude PAA. Furthermore, the bands in the $1050\text{--}900\text{ cm}^{-1}$ region could be associated to the OH deformation mode of the alcohol groups of β -CD which have not crosslinked with PAA fibers.

The FTIR gives evidence of the formation of some degree of crosslinked ester groups and other unreacted alcoholic groups from the β -CD. This is consistent with the results reported in the bibliography³⁷ and also with the high water insolubility of the thermally crosslinked fibers which has been experimentally tested by immersion in water for long periods of time (several days), while the untreated fiber mats dissolved immediately as they were rinsed gently with ultrapure water. The crosslinked fibers were stable in water, and due to the weak polyelectrolyte nature of the carboxylic groups of the PAA, they present a well known pH dependent swelling behavior.^{37,38}

Figure 4 shows two AFM images of an already crosslinked fiber mat (electrospun from a 10 wt % PAA), before and after being immersed in water for 24 h. Although it is observable a slight deformation of the fibers, they remain almost intact after the immersion time. The AFM analysis of the fiber mats shown in Figure 4 confirms the chemical and mechanical stability of the electrospun webs.

To analyze the morphology of the fibers, FE-SEM images were obtained. Figure 5 shows the diameter, distribution and thickness of these crosslinked electrospun fibers (from a 5 wt % PAA solution). In this Figure 5, it is possible to appreciate a regular morphology of the nanofibers along the coated area with some beads. Fibers, as thin as 110 nm in diameter, have been observed which provides an extremely

high active surface area to the fabricated coating. The formation of some beads with an average diameter of 500 nm in the treated area are due to the contraction of the radius of the electrospinning jet when it was driven by surface tension, see inset of Figure 5.

It is well known that the polymeric solution concentration impacts dramatically in the viscosity and consequently in the diameter of the final electrospun fibers. This is corroborated comparing the diameter of the fibers with a 5 wt % of PAA and the fibers with a 10wt % of PAA (keeping constant the β -cyclodextrin to polymer ratio). When the polymeric solution concentration is 10 wt % of PAA (Fig. 4) the electrospun fibers show an average diameter of around $2.3\text{ }\mu\text{m}$, while with the 5 wt % PAA fibers

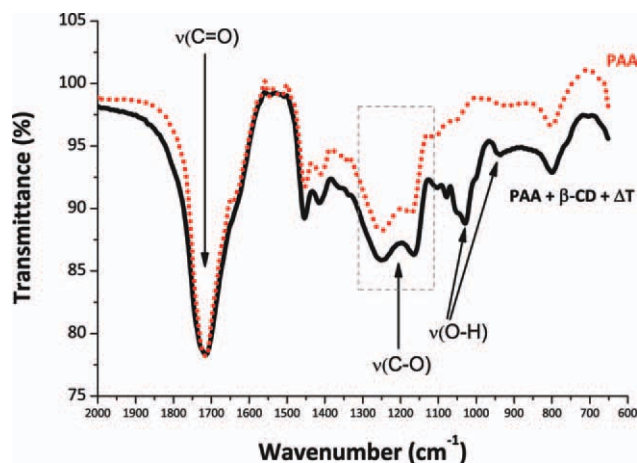


Figure 3 FTIR spectra of two different samples: PAA and PAA+ β -CD+ Δ T. [Color figure can be viewed in the online issue, which is available at [wileyonlinelibrary.com](http://www.wileyonlinelibrary.com).]

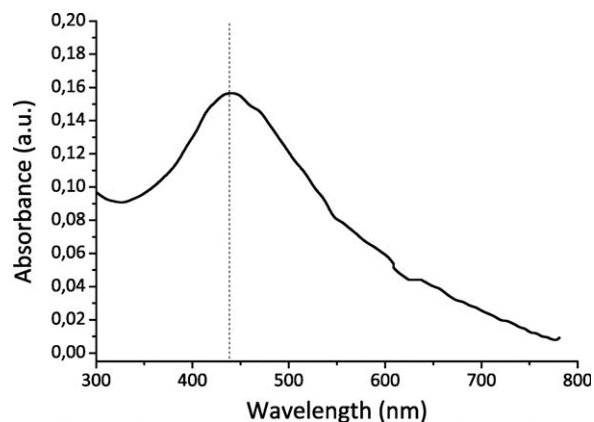


Figure 6 UV-VIS Absorption spectrum of an Ag NP loaded electrospun fiber mat.

nanoparticles is usually found around 410 nm, in this case, the NPs are packaged inside the fibers and the SPR resonant condition is red-shifted and slightly broadened.^{40,41}

It is important to remark that in other works, the silver particles are already included in the polymeric precursor solution of the electrospun fibers.^{26–29} Since it is well known that the characteristics of the final fiber mat strongly depend on the composition of the spinning solution, one of the main issues of these approaches is that the average fiber diameter and morphology can vary dramatically when parameters such as the amount of silver nanoparticles are slightly changed.⁴² Because of this, one of the main advantages of the here proposed synthesis method is that the total amount of silver loaded into the fibers can be adjusted subsequently to the fabrication of the fiber mats.

Simply by varying the number of dip/reduction cycles, or by increasing the concentration of the AgNO₃ loading solution, the nanoparticle synthesis

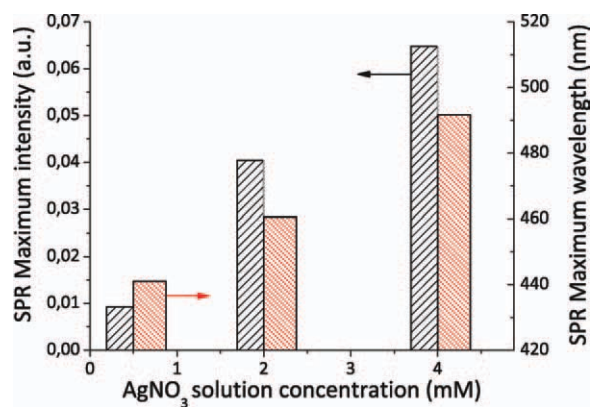


Figure 7 Variation of the intensity and the wavelength of the SPR absorption maximum depending on the concentration of the AgNO₃ loading solution. [Color figure can be viewed in the online issue, which is available at wileyonlinelibrary.com.]

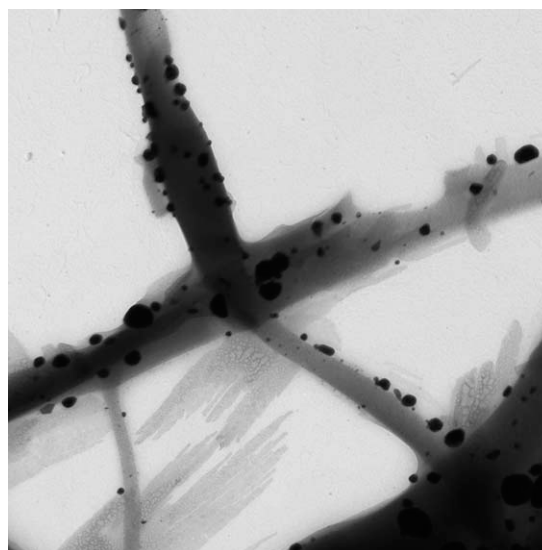


Figure 8 TEM image of the Ag NP loaded electrospun fiber mat.

is altered. In this case, the concentration of the AgNO₃ loading solution was increased while the immersion time was kept constant. The ion exchange mechanisms were more efficient, resulting in a heavier loading of Ag⁺ ions into the PAA hydrogel fibers. When those ions were reduced to Ag⁰ by immersing the fibers in DMAB, the size and aggregation of the silver nanoparticles were different depending on the loading solution concentration. This difference results in a dramatic change of the color of the fibers, observable even to the naked eye. Figure 7 shows the variation of the intensity and the peak wavelength of the SPR resonant absorption peak, as the concentration of the AgNO₃ loading solution is increased. As the amount of silver inside the fibers is higher, the SPR absorbance is stronger and the wavelength of the peak is red-shifted, in

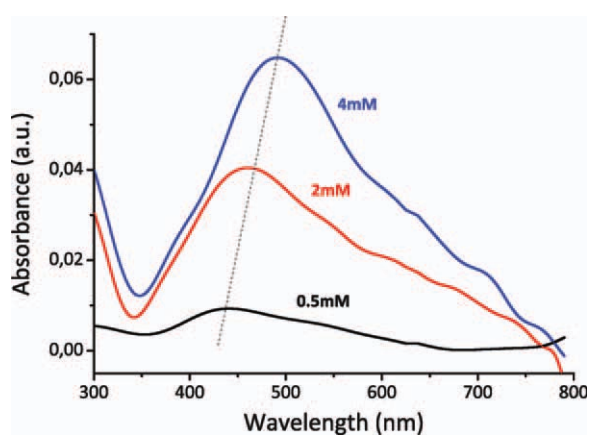


Figure 9 Variation of the absorption spectra depending on the concentration of the AgNO₃ loading solution. [Color figure can be viewed in the online issue, which is available at wileyonlinelibrary.com.]

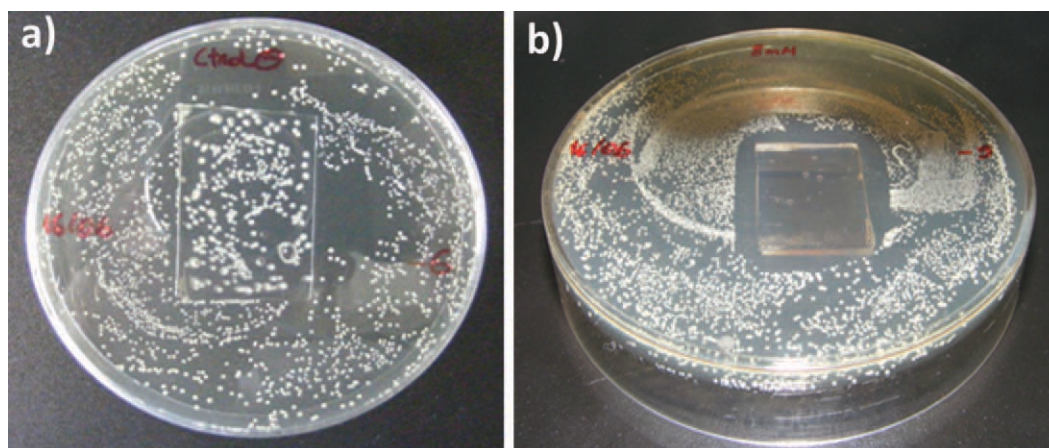


Figure 10 Bacteriological cultures of *L. plantarum* with two different samples, a reference sample with no silver nanoparticles (left) and a silver loaded electrospun fiber mat (right). [Color figure can be viewed in the online issue, which is available at wileyonlinelibrary.com.]

consonance to what it has been demonstrated in other works.^{40,41} In Figure 8, Ag NPs can be shown in the electrospun fibers by TEM micrographs.

The complete UV-VIS absorbance spectra of the samples are shown in Figure 9. This demonstrates the versatility of this approach, in which the parameters of the polymeric precursor solutions for the fabrication of the fiber membranes can be adjusted separately to optimize the nanoparticle synthesis characteristics.

Finally, the antibacterial efficiency of the fiber mats has been tested. The killing efficiency of the less loaded samples (with 0.5 mM of AgNO₃) was slightly lower than 99%, and it could not be considered biocide. Nevertheless, it has been observed a direct relation between the amount of silver contained in the electrospun fibers and their antibacterial activity. In the case of the most concentrated samples (4 mM) it is even observed an inhibition zone around the sample in which no bacterial growth was observed; therefore they show a highly efficient killing effect. In Figure 10 it is possible to see the photographs of a bare glass substrate [Fig. 10(a)] and other sample coated with electrospun fibers loaded with silver nanoparticles with a 4 mM AgNO₃ [Fig. 10(b)]. While in the reference sample the bacterial growth happened in the whole agar slab and also under the glass, in the silver loaded fibrous membrane coating no bacteria were found. The killing efficiency of these samples was higher than 99.99%.

CONCLUSIONS

In this work, silver nanoparticles were immobilized inside submicron electrospun fiber membranes and highly efficient antibacterial coatings were obtained. First, chemically stable submicron polymeric fibers

were obtained by electrospinning of PAA and β -cyclodextrin. Chemical and mechanical stable fiber mats were achieved by a thermal treatment which induced a crosslinking reaction between the PAA and the β -CD molecules. Water insoluble hydrogel-like polymeric fibers as thin as 110 nm in diameter were obtained using this technique. Afterwards, silver nanoparticles were synthesized directly within the fibers. Ag⁺ ions were loaded into the fibers via ion interchange simply by immersing the fibers into a silver nitrate solution, and then they were reduced into Ag⁰ using DMAB. The colorless fibers acquired a pale golden coloring after the reduction step, as result of the SPR absorbance peak of the silver nanoparticles. Simply by increasing the concentration of the AgNO₃ loading solution, bigger and more aggregated silver nanoparticles were obtained. The SPR absorbance peaks of the samples are red shifted in more than 80 nm and significantly increased in intensity, when the AgNO₃ loading solution concentration was varied from 0.5 to 4 mM.

Finally, the biocide effect of the silver-loaded fiber mats were tested against *Lactobacillus plantarum* bacteria. When the fiber membrane was loaded with a AgNO₃ solution more concentrated than 4 mM the coatings showed a very high killing efficiency against the bacteria, killing more than 99.99% after 24 h. Those samples even showed an inhibition zone around them.

This novel approach simplifies the fabrication protocol by allowing the separate control of the parameters of electrospinning process and the synthesis of the silver nanoparticles, giving more versatility to obtain the desired properties of the final coatings. These characteristics are an advantage over previously reported silver-loaded nanofiber mats, and this two-step process results in an efficient method to fabricate large specific surface area coatings with

a high performance biocide behavior. These fiber mats could be applied to wound healing and regeneration skin processes. To our knowledge, this is the first time that stable hydrogel nanofibers with a highly biocide behavior have been fabricated using electrospinning thanks to a two-step process which improves the reproducibility and tunability of the fiber mats.

References

1. McDonnell, G.; Russell, A. D. *Clin Microbiol Rev* 1999, 12, 147.
2. Russell, A. D. *Lancet Infect Dis* 2003, 3, 794.
3. Klasen, H. J. *Burns* 2000, 26, 117.
4. Lansdown, A. B. J. *Wound Care* 2002, 11, 125.
5. Li, W.; Xie, X.; Shi, Q.; Zeng, H.; Ou-Yang, Y.; Chen, Y. *Appl Microbiol Biotechnol* 2010, 85, 1115.
6. Bragg, P. D.; Rainnie, D. J. *Can J Microbiol* 1974, 20, 883.
7. Panáček, A.; Kolár, M.; Vecerová, R.; Pucek, R.; Soukupová, J.; Kryštof, V.; Hamal, P.; Zboril, R.; Kvítek, L. *Biomaterials* 2009, 30, 6333.
8. Travan, A.; Pelillo, C.; Donati, I.; Marsich, E.; Benincasa, M.; Scarpa, T.; Semeraro, S.; Turco, G.; Gennaro, R.; Paoletti, S. *Biomacromolecules* 2009, 10, 1429.
9. Greulich, C.; Kittler, S.; Epple, M.; Muhr, G.; Köller, M. *Langenbeck's Archives of Surgery* 2009, 394, 495.
10. Chen, X.; Schluesener, H. J. *Toxicol Lett* 2008, 176, 1.
11. Yuranova, T.; Rincon, A. G.; Bozzi, A.; Parra, S.; Pulgarin, C.; Albers, P.; Kiwi, J. *J Photochem Photobiol A* 2003, 161, 27.
12. Lee, H. Y.; Park, H. K.; Lee, Y. M.; Kim, K.; Park, S. B. *Chem Commun* 2007, 2959.
13. Gao, Y.; Cranston, R. *Text. Res. J.* 2008, 78, 60.
14. Blaker, J. J.; Nazhat, S. N.; Boccaccini, A. R. *Biomaterials* 2004, 25, 1319.
15. Sharma, V. K.; Yngard, R. A.; Lin, Y. *Adv. Colloid Interface Sci* 2009, 145, 83.
16. Sharma, J.; Imae, T. *J Nanosci Nanotechnol* 2009, 9, 19.
17. Wang, J.; Wen, L.; Wang, Z.; Chen, J. *Mater Chem Phys* 2006, 96, 90.
18. Kawashita, M.; Toda, S.; Kim, H.; Kokubo, T.; Masuda, N. *J Biomed Mater Res Part A* 2003, 66, 266.
19. Rivera-Garza, M.; Olguín, M. T.; García-Sosa, I.; Alcántara, D.; Rodríguez-Fuentes, G. *Microporous Mesoporous Mater* 2000, 39, 431.
20. Park, S.; Jang, Y. J. *Colloid Interface Sci* 2003, 261, 238.
21. Kawashita, M.; Tsuneyama, S.; Miyaji, F.; Kokubo, T.; Kozuka, H.; Yamamoto, K. *Biomaterials* 2000, 21, 393.
22. Jeon, H.; Yi, S.; Oh, S. *Biomaterials* 2003, 24, 4921.
23. Bravo, J.; Zhai, L.; Wu, Z.; Cohen, R. E.; Rubner, M. F. *Langmuir* 2007, 23, 7293.
24. Doshi, J.; Reneker, D. H. *J. Electrostatics* 1995, 35, 151.
25. Wang, X.; Drew, C.; Lee, S.; Senecal, K. J.; Kumar, J.; Samuelson, L. A. *Nano Lett* 2002, 2, 1273.
26. Melaiye, A.; Sun, Z.; Hindi, K.; Milsted, A.; Ely, D.; Reneker, D. H.; Tessier, C. A.; Youngs, W. J. *J Am Chem Soc* 2005, 127, 2285.
27. Hong, K. H.; Park, J. L.; Hwan Sul, I. N.; Youk, J. H.; Kang, T. *J. J Polym Sci Part B* 2006, 44, 2468.
28. Son, W. K.; Youk, J. H.; Park, W. H. *Carbohydr Polym* 2006, 65, 430.
29. Patel, A. C.; Li, S.; Wang, C.; Zhang, W.; Wei, Y. *Chem Mater* 2007, 19, 1231.
30. Yang, Q. B.; Li, D. M.; Hong, Y. L.; Li, Z. Y.; Wang, C.; Qiu, S. L.; Wei, Y. *Synth Met* 2003, 137, 973.
31. Jin, W.; Lee, H. K.; Jeong, R. H.; Park, W. H.; Youk, J. H. *Macromol Rapid Commun* 2005, 26, 1903.
32. Reneker, D. H.; Chun, I. *Nanotechnology* 1996, 7, 216.
33. Huang, Z.; Zhang, Y.; Kotaki, M.; Ramakrishna, S. *Compos Sci Technol* 2003, 63, 2223.
34. Nolte, A. J.; Rubner, M. F.; Cohen, R. E. *Langmuir* 2004, 20, 3304.
35. Li, Z.; Lee, D.; Sheng, X.; Cohen, R. E.; Rubner, M. F. *Langmuir* 2006, 22, 9820.
36. Urrutia, A.; Rivero, P. J.; Ruete, L.; Goicoechea, J.; Fernández-Valdivieso, C.; Arregui, F. J.; Matias, I. R. *Physica Status Solidi (C)* 2010, 7, 2774.
37. Li, L.; Hsieh, Y. *Polymer* 2005, 46, 5133.
38. Shiratori, S. S.; Rubner, M. F. *Macromolecules* 2000, 33, 4213.
39. Zan, X.; Su, Z. *Thin Solid Films* 2010, 518, 5478.
40. Yuan, W.; Ji, J.; Fu, J.; Shen, J. *J Biomed Mater Res Part B Appl Biomater* 2008, 85, 556.
41. Bhui, D. K.; Bar, H.; Sarkar, P.; Sahoo, G. P.; De, S. P.; Misra, A. *J Mol Liquids* 2009, 145, 33.
42. Hong, H.F.; Jeong, S. *J Nanosci Nanotechnol* 2011, 11, 372.